Journal of Insect Science, (2018) 18(6): 4; 1–10
doi: 10.1093/jisesa/iey098
Research

Proteomic Analysis of Larval Integument in a Dominant Obese Translucent (*Obs*) Silkworm Mutant

Lingyan Wang,[1] Zhaoming Dong,[1] Juan Wang,[1] Yaru Yin,[1] Huawei Liu,[1] Wenbo Hu,[1] Zhangchuan Peng,[1] Chun Liu,[1] Muwang Li,[2] Yutaka Banno,[3] Toru Shimada,[4] Qingyou Xia,[1] and Ping Zhao[1,5]

[1]State Key Laboratory of Silkworm Genome Biology, College of Biotechnology, Southwest University, 2 Tiansheng Road, Beibei, Chongqing 400716, China, [2]Sericultural Research Institute, Chinese Academy of Agricultural Sciences, Zhenjiang, Jiangsu 212003, China, [3]Institute of Genetic Resources, Graduate School of Bioresource and Bioenvironmental Sciences, Kyushu University, Higashi-ku, Fukuoka 812–8581, Japan, [4]Department of Agricultural and Environmental Biology, University of Tokyo, 1-1-1 Yayoi, Bunkyo-ku, Tokyo 113–8657, Japan, and [5]Corresponding author, e-mail: zhaop@swu.edu.cn

Subject Editor: Bill Bendena

Received 10 July 2018; Editorial decision 13 September 2018

Abstract

The dominant obese translucent (*Obs*) mutant of the silkworm (*Bombyx mori*) results in a short and stout larval body, translucent phenotype, and abnormal pigmentation in the integument. The *Obs* mutant also displays deficiency in ecdysis and metamorphosis. In the present study, to gain an understanding of multiple *Obs* phenotypes, we investigated the phenotypes of *Obs* and performed a comparative analysis of the larval integument proteomes of *Obs* and normal silkworms. The phenotypic analysis revealed that the *Obs* larvae were indeed short and fat, and that chitin and uric acid content were lower but melanin content was higher in the *Obs* mutant. Proteomic analysis revealed that 244 proteins were significantly differentially expressed between *Obs* and normal silkworms, some of which were involved in uric acid metabolism and melanin pigmentation. Twenty-six proteins were annotated as cuticular proteins, including RR motif-rich cuticular proteins (CPR), glycine-rich cuticular protein (CPG), hypothetical cuticular protein (CPH), cuticular protein analogous to peritrophins (CPAPs), and the chitin_bind_3 motif proteins, and accounted for over 84% of the abundance of the total significantly differentially expressed proteins. Moreover, 22 of the 26 cuticular proteins were downregulated in the *Obs* mutant. Comparative proteomic analysis suggested that the multiple phenotypes of the *Obs* mutant might be related to changes in the expression of proteins that participate in cuticular formation, uric acid metabolism, and melanin pigmentation. These results could lay a basis for further identification of the gene responsible for the *Obs* mutant. The data have been deposited to ProteomeXchange with identifier PXD010998.

Key words: dominant obese translucent, uric acid, melanin pigmentation, cuticular formation, proteomics

The integument of insects is a natural barrier covering the entire organism, which isolates internal tissues from the external environment. The integument is composed of three layers, a basement membrane in the inner layer, epidermal cells in the middle layer, and the cuticle in the outer layer. It is well known that the cuticle of insects contains a large number of cuticular proteins and chitin, and thus function as an exoskeleton to maintain insect body shape, and to protect insects from mechanical damage, dehydration, and pathogens (Andersen et al. 1995, Vincent and Wegst 2004, Guan et al. 2006).

To date, most studies on the relationship between cuticle construction and the body shape of insects have been performed in *Drosophila* (Tajiri 2017). The normal formation of body shape is affected by mutations of genes responsible for the synthesis, modification, or deposition of chitin including *krotzkopf verkehrt* (encoding chitin synthase-1) (Ostrowski et al. 2002, Moussian et al. 2005a), *mummy* (encoding UDP-*N*-acetylglucosamine pyrophosphorylase (Tonning et al. 2006), *serpentine* and *vermiform* (encoding matrix proteins with chitin binding and deacetylation domains) (Luschnig et al. 2006), *knickkopf* (a tracheal tube expansion gene) (Ostrowski et al. 2002, Devine et al. 2005), and *retroactive* (encoding a membrane-anchored extracellular protein (Moussian et al. 2005b). Muscle-related protein LIM, calmodulin7, Toll pathway components Tube and Pelle, and cuticular proteins TweedleD and Obstructor-E, have been found to be responsible for body shape in *Drosophila* (Letsou et al. 1991, Wang et al. 2003, Guan et al. 2006, Tajiri 2017, Tajiri et al. 2017). In the silkworm (*Bombyx mori*), dysfunction of cuticular proteins BmorCPR2 and BmorCPH24 results in the body

© The Author(s) 2018. Published by Oxford University Press on behalf of Entomological Society of America.
This is an Open Access article distributed under the terms of the Creative Commons Attribution-NonCommercial-NoDerivs licence (http://creativecommons.org/licenses/by-nc-nd/4.0/), which permits non-commercial reproduction and distribution of the work, in any medium, provided the original work is not altered or transformed in any way, and that the work is properly cited. For commercial re-use, please contact journals.permissions@oup.com

shape mutants *stony* and *Bo*, respectively (Qiao et al. 2014, Xiong et al. 2017). So far, about 479 silkworm mutants have been obtained and maintained as genetic resources, >20 of which are related to body shape (http://shigen.nig.ac.jp/silkwormbase/ViewStrainGroup.do, last accessed October 15, 2018). The silkworm, therefore, represents an attractive model for studying body shape determination in insects.

Dominant obese translucent (*Obs*) is one of the body shape mutants of silkworm. The *Obs* mutant not only shows a short and stout larval body shape but also exhibits a translucent phenotype and suppression of melanin deposition in the lunar, and crescent markings on the dorsal integument, as shown in Fig. 1. Moreover, abnormal phenotype is observed for *Obs* mutant in ecdysis and metamorphosis (Yoshimura et al. 1984). More than 30 mutants in silkworm exhibit the translucent phenotype (http://shigen.nig.ac.jp/silkwormbase/ViewStrainGroup.do, last accessed October 15, 2018), which results from the abnormal uric acid metabolism in the larvae (Tamura and Sakate 1983, Tamura and Akai 1990), and these mutants are termed as 'translucent mutants'. Some proteins responsible for the unique phenotype of the translucent mutants have been identified, to be involved in the biosynthesis (Kômoto 2002, Kômoto et al. 2003, Fujii et al. 2016), transport (Kômoto et al. 2009, Kiuchi et al. 2011, Wang et al. 2013b), and accumulation of uric acid (Ito et al. 2009; Fujii et al. 2010, 2012; Wang et al. 2013a; Zhang et al. 2017). The melanin pigmentation of insects has been widely studied. By the action of different enzymes, tyrosine is converted into melanogenic precursors, which are then transported from the epidermal cell into the developing cuticle, leading to the melanization of cuticles (Andersen 2010). More than 50 mutants in silkworm exhibit various larval pigmentation and patterns (Banno et al. 2010), and some of the responsible genes have been cloned (Dai et al. 2010, Futahashi et al. 2010, Ito et al. 2010, Liu et al. 2010, Zhan et al. 2010, Fujii et al. 2013, Yamaguchi et al. 2013, Yoda et al. 2014, Yuasa et al. 2016). It is notable that the content of uric acid is lower at the areas of melanin deposition in the larval integument of several lepidopteran species, and vice versa (Ninomiya et al. 2006, Hu et al. 2013). However, the biological mechanism of this phenomenon remains unknown. The *Obs* mutant is governed by a single gene but shows a pleiotropic phenotype, including abnormal body shape determination, uric acid metabolism, and melanin pigmentation (Yoshimura et al. 1984). Research on the *Obs* mutant may, therefore, provide new clues to understand the relationship among these processes in the insects.

The abnormal phenotypes of the *Obs* mutant are related to the larval integument. In this study, to gain a better understanding of the molecular mechanism determining the *Obs* phenotypes, we performed a comparative analysis of the larval integument proteomes of the *Obs* and normal silkworms on day 3 of the fifth instar using shotgun liquid chromatography–tandem mass spectrometry (LC–MS/MS). The phenotypes of *Obs* mutant were investigated, and the proteins involved in cuticle formation, uric acid metabolism, and melanin synthesis were analyzed. Our results revealed the possible reasons for the abnormal phenotypes of the *Obs* mutant, thus enhancing current understanding of the processes of body shape determination, uric acid metabolism, and melanin pigmentation, and their inter-relationships in the synthesis of insect integuments, which will provide a reference for further identification of the gene responsible for the *Obs* mutant.

Materials and Methods

Silkworm Strains and Tissue Collection

The heterozygous *Obs* mutant strain o90 (*Obs*/+) was obtained from the silkworm stock center at Kyushu University, Fukuoka, Japan. The wild-type strain p50T was obtained from the University of Tokyo. Individuals showing the *Obs* phenotype were maintained by hybridizing female offspring showing the *Obs* phenotype with p50T males (*Obs*/+♀×p50T♂). In the present study, all *Obs* and normal phenotype individuals were bred using this cross. All silkworm larvae were reared on fresh mulberry leaves at 25°C. The integuments of 3-day-old fifth-instar larvae exhibiting the normal and *Obs* phenotypes were dissected carefully on ice, and other tissues, including fat body, trachea, and head, were removed. The integuments were immediately washed with 0.7% normal saline, blotted on filter paper, and then stored at −80°C until protein extraction was performed. Three individuals with the same phenotype were collected to be one unique sample, and there were three biological replicates for each sample.

Morphological Observations and Phenotype Analysis

The integuments of the larvae showing the *Obs* and normal phenotypes on day 3 of the fifth instar were carefully dissected and treated as described earlier, cleaned with ultrapure water, blotted on filter paper, spread on plastic film, and photographed. The lengths of internodes, intersegmental folds, distances between spiracles, and circumferences at each spiracle were measured using Adobe Photoshop as described previously (Bradshaw et al. 2007).

Quantification of Chitin Content

The integuments of both *Obs* and normal phenotype larvae obtained prior to the fourth molt and on day 3 of the fifth instar were dissected and treated carefully as described earlier, cleaned with ultrapure water, and blotted on filter paper. The treated integuments and the cuticle shed during the fourth molt were dried at 60°C overnight

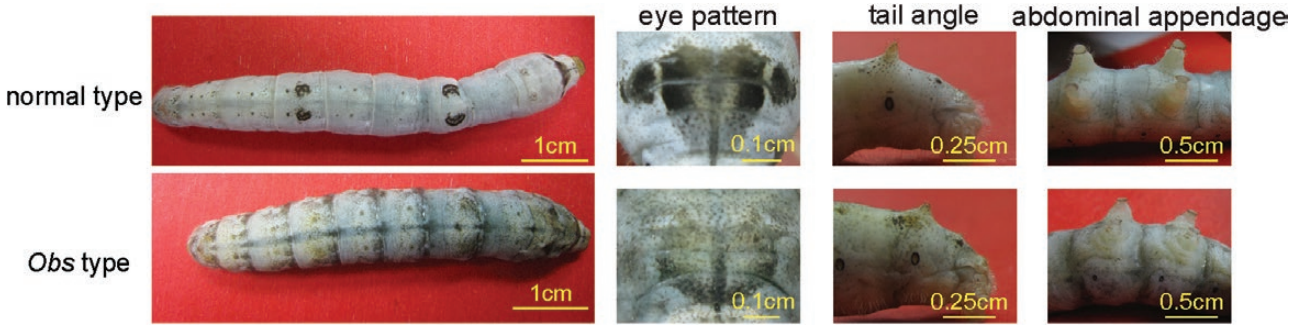

Fig. 1. Phenotype of the normal silkworm and *Obs* larvae on day 3 of the fifth instar. The normal type is indicated on the upper row, with the *Obs* type on the lower row.

and then weighed on an analytical balance (Mettler-MS105DU). Extraction and determination of chitin content were performed according to a previous protocol (Zhang and Zhu 2006). All evaluation was performed on three biological replicates for each sample.

Measurement of Uric Acid

Uric acid was extracted from integuments of 3-day-old fifth-instar larvae as described previously (Tamura 1977). The integuments were treated as described earlier, cleaned with ultrapure water, and blotted on filter paper, followed by drying at 90°C for 180 min and grinding with a pestle. Ground integument was boiled in water for 20 min; the samples were subsequently centrifuged at 12,100 × *g* at 25°C for 30 min, and the supernatant was collected. The precipitate was further treated as described earlier. Supernatants were mixed for further analysis, and uric acid was measured using a BioAssay Systems uric acid assay kit according to the manufacturer's instructions (BioAssay Systems, Hayward, CA).

Quantification of Melanin Content

The integuments of both the *Obs* and normal phenotype 3-day-old fifth-instar larvae were dissected and treated as described earlier, cleaned with ultrapure water, and blotted on filter paper. Extraction of melanin from the treated integuments was performed as described previously (Ito et al. 2016). Melanin content was estimated from a standard curve of synthetic melanin (Sigma, St. Louis, MO) at 405 nm absorbance as described previously (Sun et al. 2017). Four biological replicates of each sample were analyzed.

Protein Isolation

Samples prepared as described earlier were frozen in liquid nitrogen and ground with a pestle to produce a powder, to which an appropriate amount of SDT lysis buffer [containing 4% sodium dodecyl sulfate, 100-mM Tris/HCl pH 7.6, and 1-mM dithiothreitol (DTT)] was added . The resulting homogenate was incubated at 100°C for 15 min, followed by sonication, centrifugation (12,100 × *g*, 30 min, 4°C), and collection of the supernatant. This sodium dodecyl sulfate, dithiothreitol, and Tris/HCl (SDT) extraction processes was repeated two times, and all resulting supernatants were mixed. To this supernatant preparation, 14-ml trichloroacetic acid (TAC)/acetone (1:9) was added and the mixture was maintained at −20°C overnight. The following day, the mixture was centrifuged at 7,000 × *g* for 30 min at 4°C and the supernatant was discarded. To the pellet, 13 ml of precooled acetone was added followed by centrifugation at 7,000 × *g* for 30 min. This acetone wash procedure was repeated three times and the final pellet was air-dried. An appropriate amount of SDT lysis buffer was added to the dried pellet, followed by mixing and boiling for 15 min. The preparation was centrifuged at 14,000 × *g* for 40 min and the supernatant was collected. Proteins in the supernatant were quantified using a BCA Protein Assay Kit (Bio-Rad, Hercules, CA). Remaining sample was stored at −80°C for further experiments.

Protein Digestion

Proteins purified above were digested according to the FASP procedure (Wiśniewski et al. 2009). For each sample, 200 µg of protein solution was reduced by incubation with 100-mM DTT in a boiling water bath for 15 min, and cooled to room temperature. To this solution, 200-µl urea (UA) buffer (8M urea, 150 mM Tris–HCl, pH 8.0) was added, followed by thorough mixing. The mixture was then transferred to 30-kDa ultrafiltration centrifuge tubes (Wiśniewski et al. 2009) and centrifuged at 14,000 × *g* for 15 min. After discarding the flow-through, 200-µL UA buffer was added, followed by centrifugation at 14,000 × *g* for 15 min, and again discarding the flow-through. Thereafter, 100-µl iodoacetamide (IAA) (50 mM IAA in UA) was added to alkylate the preparation, followed by oscillation at 600 rpm for 1 min. The preparation was then stored in the dark for 30 min at room temperature and centrifuged at 14,000 × *g* for 10 min. The ultrafiltration tube was washed twice with 100-µl UA buffer and then twice with 100-µl 25 mM NH_4HCO_3. Proteins were digested with trypsin (2-µg trypsin in 40-µl NH_4HCO_3 buffer) overnight at 37°C. Since the digested peptides were smaller than the bore diameter of the super filter, tryptic peptides were collected by centrifugation at 14,000 × *g* for 10 min, after which the tryptic peptides were desalted on a C18-SD Extraction Disk Cartridge (66872-U Sigma). The peptide content was estimated by UV light spectral density at 280 nm.

Liquid Chromatography-Tandem Mass Spectrometry Analysis

Equal amounts of tryptic peptides for each example were separated using a Thermo Finnigan EASY-nLC 1000 system (Thermo Fisher Scientific, Waltham, MA). The peptide mixture was loaded into a Thermo EASY column SC001 trap (150 µm × 20 mm; RP-C_{18}) connected to a Thermo EASY column SC200 150 µm × 100 mm (RP-C_{18}) in mobile phase A (0.1% formic acid in 2% acetonitrile), and separated with a linear gradient of 0%–100% mobile phase B (0.1% formic acid in 84% acetonitrile) over 120 min at a flow rate of 400 nl/min. LC–MS/MS analysis was performed for 120 min using a Q-Exactive mass spectrometer (Thermo Fisher Scientific). MS data were acquired using a data-dependent top10 method, dynamically selecting the most abundant precursor ions from the survey scan (300–1,800 m/z) with a charge state of +2 to +5 for higher collisional dissociation (HCD) fragmentation. The duration dynamic exclusion was 60 s. Survey scans were acquired at a resolution of 70,000 at m/z 200 and the resolution for HCD spectra was set to 17,500 at m/z 200, and with an isolation width of 2 m/z. The normalized collision energy was 30 eV.

Protein Identification and Label-Free Quantification

Six raw LC–MS/MS files obtained from the above process were analyzed using MaxQuant version 1.3.0.5 (Max Planck Institute of Biochemistry, Martinsried, Germany) (Cox and Mann 2008). The MaxQuant searches were performed against the Silkworm Genome Database (SilkDB) (http://silkworm.swu.edu.cn/silkdb/, last accessed October 15, 2018), National Center for Biotechnology Information (https://www.ncbi.nlm.nih.gov/, last accessed October 15, 2018), and KAIKObase (http://sgp.dna.affrc.go.jp/KAIKObase/, last accessed October 15, 2018) databases. Peptide searches were executed using Andromeda search algorithms (Cox et al. 2011). Main search and MS/MS tolerance precursors were set to 6 and 20 ppm, respectively. Two missed cleavages were allowed. Methionine oxidation and N-terminal acetylation were used as the variable modifications, and carbamidomethylation of cysteines was considered a fixed modification. For all searches, the false discovery rate of peptide and protein identifications was 1%. The minimum number of quantified peptides per protein was one unique peptide. Proteins that were detected in two or more biological replicates were considered as representing reliable results. The data have been deposited to the ProteomeXchange Consortium via the PRIDE partner repository with the dataset identifier PXD010998. The identified peptides and proteins are listed in Supp Tables 1 and 2 (online only), respectively. For the following analyses, all common contaminants were removed.

For comparison of protein abundances across different samples, the label-free quantification (LFQ) algorithm was used, which compares the intensities of the same peptides detected in different samples (Luber et al. 2010). In contrast, for comparison of abundances of different proteins within a sample, the intensity-based absolute quantification (iBAQ) algorithm was used (Schwanhäusser et al. 2011). The ratio of LFQ intensity of the *Obs* type compared with that of the normal type was set at two times as the criteria for screening significantly differential proteins with a statistically significant difference (P-value < 0.05). Statistical differences were evaluated using a t-test.

Results

Characterization of the *Obs* Mutant

Obs larvae have many different phenotypic characteristics when compared with the normal silkworm phenotype, including a short and stout larval body shape, translucent phenotype, abnormal melanin pigmentation, a shorter tail angle and abdominal appendage, and a lighter eye pattern (Fig. 1). Both *Obs* and normal-type larvae have 3 thoracic segments and 10 abdominal segments. By measuring the lengths of the internodes, intersegmental folds, and spiracles spacing in abdominal segments according to Supp Fig. 1 [online only], we found that the body shape of *Obs* larvae is consistently shorter (Fig. 2A–C). By measuring the circumference at each spiracle, we found that the circumference at the third, eighth, and ninth spiracles of *Obs* larvae was significantly greater than that of the normal type, although the circumference at the other spiracles did not differ significantly between the two types (Fig. 2D). This helps explain why *Obs* larvae appear slightly fatter than the normal-type larvae. These findings indicate that *Obs* larvae are indeed short and fat.

Determination of Chitin, Uric Acid, and Melanin Content

Chitin is a principal cuticle component and is crucial for the growth and development of insects. Chitin content was, therefore, determined in the larval integuments before the fourth molt, on day 3 of the fifth instar, and in the cuticle shed during the fourth molt. The results indicated that the content of chitin was significantly lower during these three periods in *Obs* larvae (Fig. 3A).

Although *Obs* is regarded as a translucent mutant, *Obs* individuals lack the appearance of the classical translucent mutants of silkworm described in previous studies (Kiuchi et al. 2011, Wang et al. 2013a,b). By determining the uric acid content in the larval integument of *Obs* and normal-type larvae, we found that the content

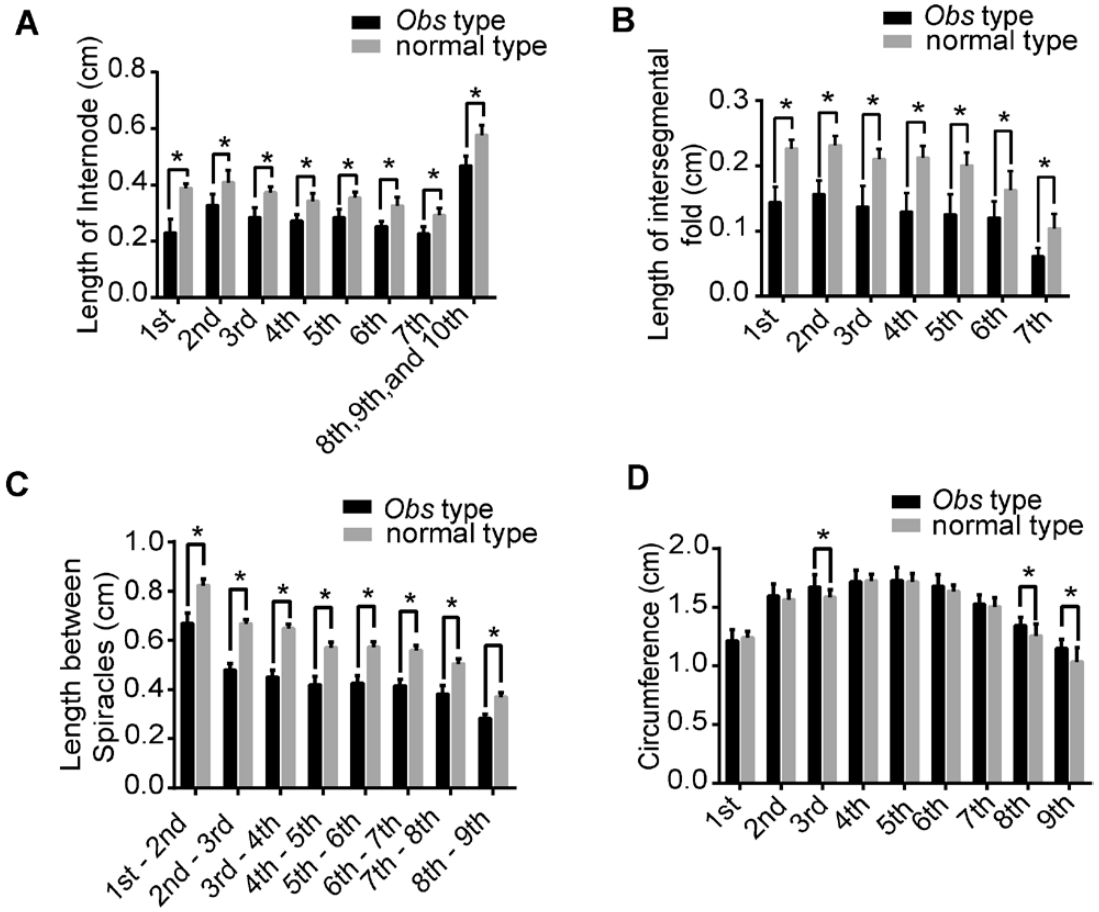

Fig. 2. Characterization of the *Obs* mutant. (A) Length of internodes in the abdominal segment of the normal type and *Obs* type. 1st indicates the first abdominal internode, 2nd indicates the second abdominal internode, and so on. The eighth, ninth, and tenth internodes were measured as one internode because it is difficult to measure them separately. $n = 15$. (B) Length of intersegmental folds in the abdominal segment of the normal type and *Obs* type. 1st indicates the first intersegmental fold, 2nd indicates the second intersegmental fold, and so on. $n = 15$. (C) Length between spiracles of the normal type and *Obs* type. '1st–2nd' indicates between the first and second spiracles, '2nd–3rd' indicates between the second and third spiracles, and so on. $n = 15$. (D) Circumference at each spiracle of the normal type and *Obs* type. 1st indicates the first spiracle, 2nd indicates the second spiracle, and so on. $n = 15$. Data are presented as means ± SD. Student's t-test, * $P < 0.05$ (A–D).

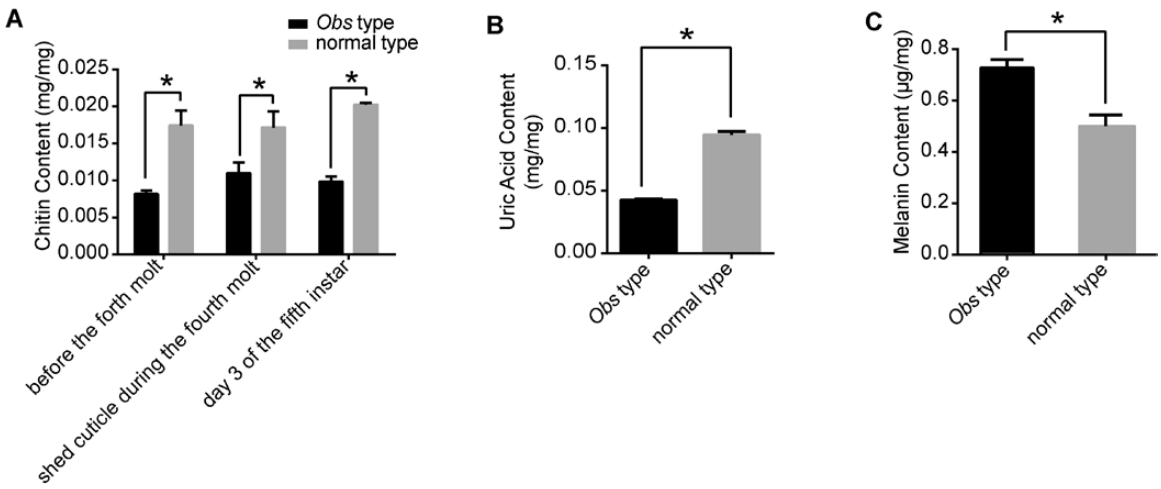

Fig. 3. Assay of chitin, uric acid, and melanin content. (A) Content of chitin in the larval integuments before the fourth molt, the cuticle shed during the fourth molt, and the integuments on day 3 of the fifth instar, $n = 3$. (B) Content of uric acid in the larval integuments of *Obs* and normal type on day 3 of the fifth instar, $n = 3$. (C) Content of melanin in the larval integuments of *Obs* and normal type on day 3 of the fifth instar, $n = 4$. mg/mg indicates the content of chitin and uric acid in the 1 mg larval integuments. μg/mg indicates the content of melanin in the 1 mg larval integuments. Data are presented as mean ± SD. Student's *t*-test, * $P < 0.05$ (A–C).

was significantly lower in the larval integument of *Obs* (Fig. 3B), indicating that *Obs* is a true translucent mutant.

The body color of *Obs* larvae appears darker than that of the normal type. We speculated that there was a difference in the melanin content in integuments of *Obs* and normal-type larvae on day 3 of the fifth instar, and the results showed that the melanin content in the larval integument of *Obs* was significantly higher than that of the normal type (Fig. 3C). This may be the reason why the body color of *Obs* becomes darker than that of normal-type larvae.

Total Proteins and Differential Protein Expression

The *Obs* mutant not only exhibits an abnormal body shape but also shows reduced accumulation of uric acid and abnormal pigmentation in the larval integuments. To elucidate the cause of multiple phenotypes, we performed LC–MS/MS analyses on the total proteins of *Obs* and normal-type integument on day 3 of the fifth instar. Taking all data together, we identified 16,010 tryptic peptides (Supp Table 1 [online only]). These peptides were assembled into 2,131 proteins (Supp Table 2 [online only]), among which 1,981 proteins were common to *Obs* and normal-type larvae, whereas only 117 and 33 were identified exclusively in *Obs* and normal type larvae, respectively (Fig. 4, Supp Table 3 [online only]). In total, 1,380 proteins were differentially expressed between *Obs* and normal-type larvae (Fig. 4, Supp Table 4 [online only]), among which 53 were significantly upregulated and 41 were significantly downregulated in the *Obs* larvae compared with the normal-type larvae (Fig. 4, Supp Table 5 [online only]). Overall, 244 proteins showed significantly differential expression between *Obs* and normal-type larvae, and the following analyses were performed on the basis of these differentially expressed proteins.

Classification of Significantly Differentially Expressed Proteins

The 244 significantly differentially expressed proteins between *Obs* and normal-type larvae were classified into 10 categories based on their annotated molecular function: enzymes (109), cuticular proteins (26), cytoskeleton-related proteins (20), small molecule- and ion-binding and transport proteins (21), protein synthesis-related

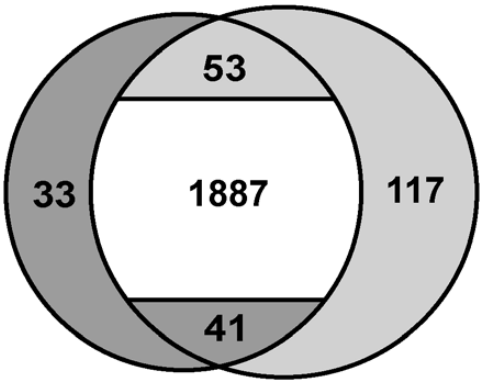

Fig. 4. Statistics of protein groups in Venn diagrams. 33 = proteins only identified in the normal-type larvae. 117 = proteins only identified in *Obs* larvae. 53 = proteins significantly upregulated and 41 = proteins significantly down-regulated in the *Obs* larvae. 1,887 = proteins not significantly up- or downregulated between *Obs* and normal-type larvae. LFQ intensity of *Obs* type/ LFQ intensity of normal type (Ratio) >2 or <0.5 and $P < 0.05$ were set as the criteria for screening significantly differential proteins. Deep gray color indicates proteins not identified or significantly downregulated in the *Obs* type. Light gray color indicates proteins only identified or significantly upregulated in the *Obs* type.

proteins (15), vesicular transport-related proteins (12), nutrient storage proteins (7), protease inhibitors (5), immune-related proteins (11), and nonclassified and unknown-function proteins (18) (Fig. 5A; Supp Table 6 [online only]). The detected enzymes included six subgroups (EC1–6), of which oxidoreductases (EC1, 27%), transferases (EC2, 22%), and hydrolases (EC3, 27%) comprised 76% of the total number of enzymes. The cuticular proteins are mainly chitin-binding structural proteins. The cytoskeleton-related proteins are actin, tubulin, and their binding proteins. The small molecule- and ion-binding and transport proteins are involved in the interaction with carbohydrates, lipids, ions, and other small molecules. The category of protein synthesis-related proteins consists of replication-, transcription-, and translation-related proteins. The vesicular transport-related proteins are involved in processes mediated by transport vesicles. The nutrient storage proteins mainly belong to the low molecular mass

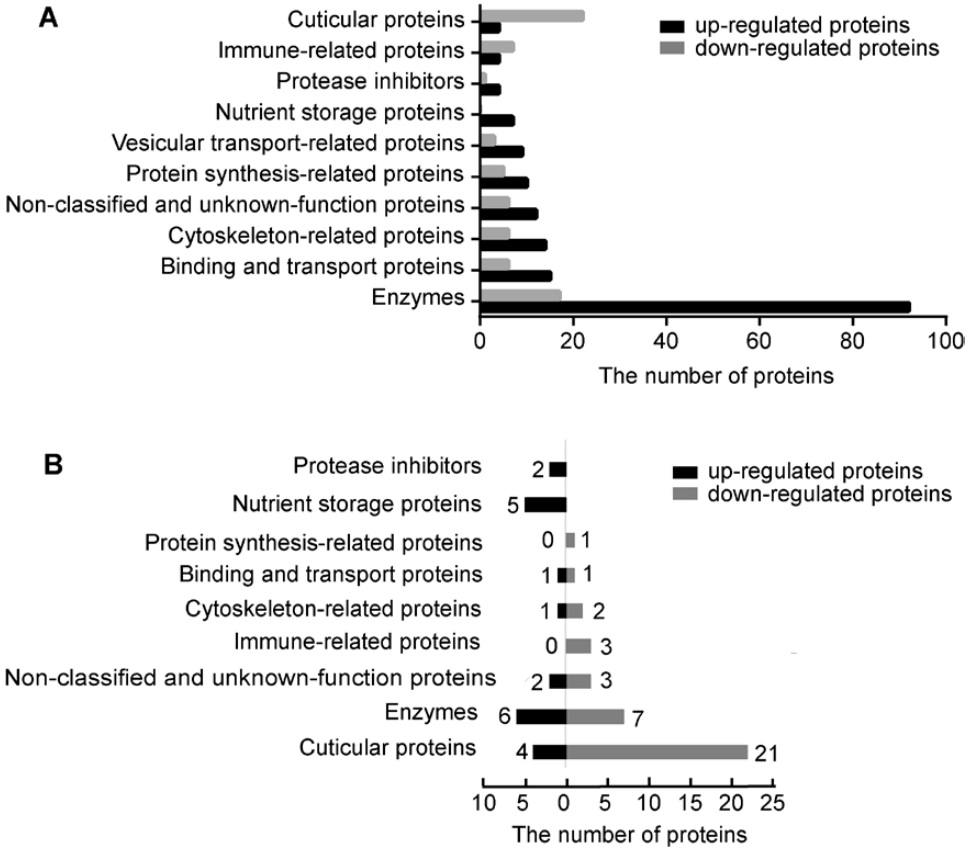

Fig. 5. Analysis of significantly different proteins. (A) Protein categorization based on annotated molecular function. (B) Chitin-binding protein categorization based on annotated molecular function. Binding and transport proteins indicate small molecule- and ion-binding and transport proteins. The abscissa (*x*-axis) shows the number of proteins mapped to each categorization. Bars indicate the number of proteins.

30-kDa lipoproteins. The identified protease inhibitors are classified into the serpin family and cysteine-rich protease inhibitor families.

Analysis of Chitin-Binding Proteins

Chitin-binding proteins play key roles in the structural and functional integrity of the cuticle. Figure 3A shows that the content of chitin was significantly reduced in *Obs* at the sampling time points employed in the present study. Therefore, we analyzed differences in the expression of chitin-binding proteins between *Obs* and normal-type larvae. According to a previous report (Dong et al. 2016), chitin-binding proteins mainly include cuticular proteins, 30-kDa lipoproteins, enzymes, and some small molecule-binding and transport proteins. Here, in our work, 59 proteins of the 244 significantly differentially expressed proteins were identified as chitin-binding proteins (Fig. 5B and Supp Table 7 [online only]). Among these, 21 proteins were significantly upregulated and 38 were significantly downregulated in the *Obs* larvae compared with the normal-type larvae. Of these 59 proteins, the highest proportion (42%) was cuticular proteins.

In the present study, the expression of 26 cuticular proteins was identified to be significantly altered between *Obs* and normal-type larvae, with four being upregulated and 22 being downregulated in *Obs* (Table 1). According to the classification of cuticular proteins (Dong et al. 2016), 16 out of the 26 cuticular proteins belonged to the RR motif-rich cuticular proteins (CPR), 5 were glycine-rich cuticular proteins (CPG), 2 were hypothetical cuticular proteins (CPH), and 2 were CPAP families, and 1 was chitin_bind_3 motif, as shown in Table 1. With the exception of one CPG motif protein, BGIBMGA010654, other cuticular proteins were identified as chitin-binding proteins. Furthermore, we estimated the protein abundance using the iBAQ algorithm (Supp Tables 8 and 9 [online only]). The results showed that the abundance of the 26 cuticular proteins and the total proteins were reduced in *Obs* larvae, and the abundance of these cuticular proteins in *Obs* larvae represented only 56.5% of that in the normal type larvae (Fig. 6). In addition, we found that the abundance of cuticular proteins accounted for 84.3% and 94.0% of the total proteins in *Obs* and normal type larvae, respectively (Fig. 6).

Analysis of Proteins Related to the Translucent Mutants in Silkworm

To date, the genes responsible for 10 translucent mutants in silkworm have been cloned as described in the Introduction. In the present study, we analyzed the proteins encoded by these 10 genes. The results showed that only the protein responsible for the *os* translucent mutant, BGIBMGA003864, was significantly downregulated in *Obs* individuals (Kiuchi et al. 2011; Supp Fig. 2A [online only]). In addition, the protein responsible for another silkworm translucent mutant, *ow* (BGIBMGA000173) (Ito et al. 2009), was downregulated by approximately 1.90-fold (Supp Fig. 2B [online only]); however, it did not meet the criterion (ratio: >2 or <0.5) used when screening for significantly differentially expressed proteins.

Analysis of Proteins Related to Melanin Synthesis

The *Obs* mutant is characterized by abnormal pigmentation on the lunar and crescent markings, and eye pattern as shown in Fig. 1.

Table 1. Cuticular proteins differentially expressed significantly between the *Obs* and normal-type larvae

Protein IDs	LFQ intensity average of *Obs* type	LFQ intensity average of normal type	Ratio (*Obs*/normal) type	*P*-value	Cuticular protein family
BGIBMGA010500	3.77E + 08	1.09E + 08	3.47	5.43E – 03	CPR
BGIBMGA010913	2.47E + 10	1.18E + 10	2.10	6.11E – 05	CPR
BGIBMGA000339	3.00E + 07	0			CPR
BGIBMGA012605	5.73E + 07	0			CPR
BGIBMGA000249	7.81E + 09	1.58E + 10	0.49	2.60E – 04	CPR
BGIBMGA013163	1.45E + 09	3.44E + 09	0.42	9.72E – 03	CPR
BGIBMGA000324	6.61E + 09	2.39E + 10	0.28	7.39E – 03	CPR
BGIBMGA012594	7.05E + 08	1.61E + 09	0.44	3.83E – 03	CPR
BGIBMGA002549	1.50E+10	4.90E + 10	0.31	2.60E – 03	CPR
BGIBMGA000332	2.80E + 09	6.12E + 09	0.46	2.48E – 03	CPR
BGIBMGA000329	6.07E + 10	1.70E + 11	0.36	8.25E – 04	CPR
BGIBMGA000333	1.54E + 10	3.98E + 10	0.39	2.52E – 04	CPR
BGIBMGA000338	8.78E + 08	2.06E+09	0.43	2.51E – 04	CPR
BGIBMGA012596	6.94E + 08	2.87E + 09	0.24	1.11E – 04	CPR
BGIBMGA005278	1.71E + 10	5.10E + 10	0.33	1.82E – 02	CPR
BGIBMGA014015	0	1.55E+07			CPR
BGIBMGA000330	1.22E + 09	2.68E + 09	0.46	2.62E – 05	CPG
BGIBMGA002385	5.32E + 08	1.95E + 09	0.27	3.05E – 03	CPG
BGIBMGA008213	5.92E + 08	1.87E + 09	0.21	4.40E – 03	CPG
BGIBMGA008255	6.99E + 09	2.74E + 10	0.25	2.26E – 04	CPG
BGIBMGA010654	0	7.41E + 07			CPG
BGIBMGA011141	0	1.61E + 08			Chitin_bind_3
BGIBMGA014292	9.91E + 09	2.28E + 10	0.43	2.16E – 03	CPH
gi|223670968|	3.92E + 09	8.60E + 09	0.46	3.98E – 03	CPH
BGIBMGA007901	1.76E + 08	4.72E + 08	0.37	9.00E – 03	CPAP
BGIBMGA007677	7.55E + 09	1.76E + 10	0.43	9.06E – 04	CPAP

Note: All cuticular proteins except BGIBMGA010654 have chitin-binding ability.

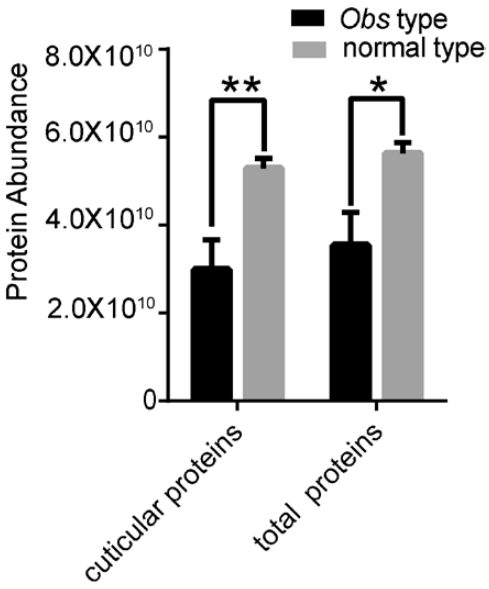

Fig. 6. Abundance analysis of significantly differentially expressed proteins. Total proteins indicate the total significantly differentially expressed proteins. The data are presented as means ± SD. ($n = 3$), Student's *t*-test, $^{**}P < 0.01$,$^{*}P < 0.05$.

Figure 3C also showed that the melanin content in the integument of *Obs* larvae was significantly higher than that of the normal type. Analysis of the proteins related to melanin synthesis revealed that BGIBMGA003199 and gi\|827552989\|, which were annotated as dopa decarboxylase and phenoloxidase subunit 1-like, respectively, appeared to be significantly upregulated (Supp Fig. 2C and D [online only]).

Analysis of *Obs* Mutant Candidate Genes

The *Obs* mutant is governed by a single gene, which has been mapped at 6.2 cM on chromosome 18 (Yoshimura et al. 1984). In this study, the 244 significantly differentially expressed proteins were detected between the *Obs* mutant and normal silkworm, indicating that the mutation of the *Obs* gene could alter the expression of these proteins. To identify the possible candidate gene, the loci of genes encoding the 244 significantly differentially expressed proteins were analyzed according to reference genomes (http://silkworm.swu.edu.cn/silkdb/ and http://silkbase.ab.a.u-tokyo.ac.jp/cgi-bin/index.cgi, last accessed October 15, 2018) (Supp Tables 3 and 5 [online only]). The results indicated that nine genes encoding significantly differentially expressed proteins were located on chromosome 18 (Supp Table 10 [online only]) and were, therefore, potential candidate genes for the *Obs* mutant. Among these nine genes, *BGIBMGA008213* and *BGIBMGA008255* encode cuticular proteins. The proteins encoded by *AK383678* and *gi\|827551453\|* are methylmalonate-semialdehyde dehydrogenase and 4-coumarate-CoA ligase 1-like, respectively. The protein encoded by *gi\|512914799\|* was annotated as an odorant-binding protein, which has been shown to be essential for a normally functioning olfactory system (Brito et al. 2016). *BGIBMGA008525* is the silkworm homologue of the human gene encoding glutaredoxin-related protein 5, which has been reported to be related to oxidative stress (Ananthi et al. 2008, Linares et al. 2009). A myofilin protein encoded by *gi\|226903597\|* has been reported to be involved in the formation of the thick filaments of insect muscle (Qiu et al. 2005). *BGIBMGA008477* is a silkworm homologue of the gene encoding 39S ribosomal protein L17, which is known to be involved in the process of translation, and has been reported to be a noninvasive biomarker with potential value in the differential diagnosis of minimal change disease and primary

focal segmental glomerulosclerosis (Pérez et al. 2017). The protein encoded by *BGIBMGA008526* is a protein of unknown function.

Discussion

Obs is a pleiotropic mutant of silkworm showing multiple phenotypes. The body of mutant larvae is short, stout, and translucent. Furthermore, there is an absence of melanin pigmentation on the lunar and crescent markings on the second- and fifth-abdominal segments, respectively. *Obs* larvae experience deficiency in completing ecdysis and metamorphosis (Yoshimura et al. 1984). In this study, we observed that the eye pattern color of *Obs* larvae was lighter, and the tail angle and abdominal appendages were shorter than those of the normal-type larvae. In order to gain an understanding of the molecular processes underlying these abnormalities in the *Obs* mutant, we analyzed differences in the proteomes of *Obs* and normal-type larval integuments on day 3 of the fifth instar using LC–MS/MS, thus expanding current knowledge of the body shape determination, the metabolism of uric acid, and integument pigmentation in the silkworm.

The body shape of *Obs* larvae is shorter and stouter than that of the normal-type larvae. The *Obs* mutant gene has been located on Chromosome 18 (Yoshimura et al. 1984). In this study, 26 cuticular proteins were significantly differentially expressed between *Obs* and the normal-type larvae. Two of these are encoded by *BGIBMGA008213* and *BGIBMGA008255*, which are located on chromosome 18. The silkworm genome contains about 220 genes encoding cuticular proteins (Futahashi et al. 2008). Until now, the mutation of only two cuticular protein genes has been known to produce mutated body shape in silkworm. For example, dysfunction in BmorCPR2 arising from a frame shift mutation in the silkworm *stony* mutant, results in an abnormal body shape with the limitation of cuticle extension and an aberrant ratio between internodes and intersegmental folds. At the same time, reduced chitin content in larval cuticle was discovered in the *stony* mutant (Qiao et al. 2014). *Bo*, another mutant, exhibits a bamboo-like body shape because of a 5-bp deletion in the second exon of *BmorCPH24* that results in a frame shift mutation (Xiong et al. 2017). Furthermore, in *Drosophila*, cuticular proteins, TweedleD and Obstructor-E, have been found to be responsible for body shape (Guan et al. 2006, Tajiri et al. 2017). These findings indicate that gene mutation of cuticular proteins can result in body shape mutations in insects. Thus, we infer that the unique phenotype of the *Obs* mutant might be caused by one of the two cuticular protein genes. Regarding the high number of cuticular proteins differentially expressed in the *Obs* mutant, we speculated that the mutation in a cuticular protein gene might cause the abnormal formation of the *Obs* larval cuticle, which influenced the expression of other cuticular proteins. Alternatively, the mutation of other genes, such as those encoding transcription factors or signaling molecules, may lead to changes in downstream genes encoding cuticular proteins, thus resulting in the *Obs* mutant phenotypes.

The *Obs* mutant not only shows a short and stout larval body shape but also experiences deficiency in completing ecdysis and metamorphosis (Yoshimura et al. 1984). Chitin is one of the main components of the cuticle and is essential for the structural and functional integrity of cuticle (Moussian et al. 2005a). For example, chitin deficiency leads to a weakened cuticle in *Tribolium castaneum* embryos (Arakane et al. 2008). In *Drosophila* embryos, deficiency of chitin also causes the softening of cuticle (Moussian et al. 2005a). In this study, the reduction of chitin was detected in the larval cuticle of *Obs* mutant. It is possible that the cuticle structure in *Obs* mutant was disrupted due to a shortage of chitin, which resulted in inability of ecdysis and metamorphosis. In addition, the deacetylation of chitin is required for the cross-linking of proteins via amino groups, which renders the insect cuticle rigid and compact (Zhu et al. 2016, Qu et al. 2017). In this study, 59 significantly differentially expressed proteins were identified to have chitin-binding abilities according to a previous report (Dong et al. 2016). Two of these, gil160333138| and BGIBMGA006214, are the homologous proteins of chitin deacetylase 1 and 2 in silkworm (Supp Fig. 2E and F [online only]). It has been reported that the downregulation of chitin deacetylase 1 and 2 resulted in an inability to shed the old cuticle; consequently, the mutant were found trapped in their exuviae, in the case of *T. castaneum* (Arakane et al. 2009, Zhu et al. 2016). It is, therefore, possible that the downregulation of these two proteins may cause a reduction in chitin deacetylation in *Obs* larvae, leading to the difficulty in completing ecdysis and metamorphosis.

The silkworm translucent mutant *os* is known to be defective in a gene encoding a hypothetical uric acid transporter in epidermal cells (Kiuchi et al. 2011). In the present study, BGIBMGA003864, the protein responsible for *os*, was significantly downregulated in *Obs* (Supp Fig. 2A [online only]) and may contribute to the translucent phenotype of *Obs*. In addition, another silkworm translucent mutant, *ow*, is controlled by Bmvarp, which is homologous to the vacuolar protein for sorting domain-containing proteins in mammals (Ito et al. 2009). In this study, BGIBMGA000173, which is responsible for *ow*, was downregulated by approximately 1.9-fold (Supp Fig. 2B [online only]). The downregulation of this protein may also contribute to the translucent phenotype of *Obs*.

Although our results showed that the melanin content in *Obs* larvae was significantly higher than that in normal-type larvae, light eye spots were observed, and crescents and star spots were barely visible in *Obs*. It has been reported that the pigmentation of larval cuticle markings in the swallowtail butterfly, *Papilio xuthus*, is closely related to the structures of the cuticle (Futahashi et al. 2012). Similarly, a correlation between the scale structure and pigmentation in butterfly wings has been reported (Janssen et al. 2001). This work showed that the reduction of chitin could disrupt the structural integrity of cuticle in the *Obs* mutant. It is possible that the defective structure of the larval cuticle may be an important reason for the abnormal melanin pigmentation in *Obs* larvae. In addition, in *P. xuthus*, several cuticular proteins display pigment-marking specificity and have been speculated function in transporting or maintaining specific cuticular pigments (Futahashi et al. 2012). Some of the downregulated cuticular proteins in *Obs* may, therefore, be involved in the transportation of the melanin or maintenance of melanin pigmentation.

Conclusions

The *Obs* mutant is a dominant mutant controlled by a single gene and is associated with multiple phenotypes. In this study, we investigated the phenotypes of *Obs* and analyzed the differential protein expression between the larval integument of *Obs* and normal silkworms. Comparative proteomic analysis suggested that the multiple phenotypes of *Obs* were related to the changes in the expression of proteins that participate in cuticle formation, uric acid metabolism, and melanin pigmentation. These observations may substantially contribute to understanding the molecular mechanisms underlying the *Obs* phenotypes.

Supplementary Data

Supplementary data are available at *Journal of Insect Science* online.

Acknowledgments

The silkworm strain *Obs* used in this study was kindly provided by the National Bio-Resource Project (NBRP) of the Ministry of Education, Culture, Sports, Science and Technology in Japan (MEXT). We acknowledge the technicians of Shanghai Applied Protein Technology Co. Ltd, who performed label-free quantitative proteomic analysis.

Funding

This work was supported by the National Natural Science Foundation of China (31401048), Chongqing Research Program of Basic Research and Frontier Technology (cstc2014jcyjA80007 and cstc2017jcyjAX0090), and Fundamental Research Funds for the Central Universities of China (XDJK2014B017 and XDJK2017D114).

Competing interests

All authors declare that they have no conflict of interest.

References Cited

Ananthi, S., T. Chitra, R. Bini, N. V. Prajna, P. Lalitha, and K. Dharmalingam. 2008. Comparative analysis of the tear protein profile in mycotic keratitis patients. Mol. Vis. 14: 500–507.

Andersen, S. O. 2010. Insect cuticular sclerotization: a review. Insect Biochem. Mol. Biol. 40: 166–178.

Andersen, S. O., P. Højrup, and P. Roepstorff. 1995. Insect cuticular proteins. Insect Biochem. Mol. Biol. 25: 153–176.

Arakane, Y., C. A. Specht, K. J. Kramer, S. Muthukrishnan, and R. W. Beeman. 2008. Chitin synthases are required for survival, fecundity and egg hatch in the red flour beetle, *Tribolium castaneum*. Insect Biochem. Mol. Biol. 38: 959–962.

Arakane, Y., R. Dixit, K. Begum, Y. Park, C. A. Specht, H. Merzendorfer, K. J. Kramer, S. Muthukrishnan, and R. W. Beeman. 2009. Analysis of functions of the chitin deacetylase gene family in *Tribolium castaneum*. Insect Biochem. Mol. Biol. 39: 355–365.

Banno, Y., T. Shimada, Z. Kajiura, and H. Sezutsu. 2010. The silkworm-an attractive bioresource supplied by Japan. Exp. Anim. 59: 139–146.

Bradshaw, J., M. E. Rice, and J. W. Hill. 2007. Digital analysis of leaf surface area: effects of shape, resolution, and size. J. Kansas. Entomol. Soc. 80: 339–347.

Brito, N. F., M. F. Moreira, and A. C. Melo. 2016. A look inside odorant-binding proteins in insect chemoreception. J. Insect Physiol. 95: 51–65.

Cox, J., and M. Mann. 2008. MaxQuant enables high peptide identification rates, individualized p.p.b.-range mass accuracies and proteome-wide protein quantification. Nat. Biotechnol. 26: 1367–1372.

Cox, J., N. Neuhauser, A. Michalski, R. A. Scheltema, J. V. Olsen, and M. Mann. 2011. Andromeda: a peptide search engine integrated into the MaxQuant environment. J. Proteome Res. 10: 1794–1805.

Dai, F. Y., L. Qiao, X. L. Tong, C. Cao, P. Chen, J. Chen, C. Lu, and Z. H. Xiang. 2010. Mutations of an arylalkylamine-*N*-acetyltransferase, *Bm-iAANAT*, are responsible for silkworm melanism mutant. J. Biol. Chem. 285: 19553–19560.

Devine, W. P., B. Lubarsky, K. Shaw, S. Luschnig, L. Messina, and M. A. Krasnow. 2005. Requirement for chitin biosynthesis in epithelial tube morphogenesis. Proc. Natl. Acad. Sci. USA 102: 17014–17019.

Dong, Z. M., W. W. Zhang, Y. Zhang, X. L. Zhang, P. Zhao, and Q. Y. Xia. 2016. Identification and characterization of novel chitin-binding proteins from the larval cuticle of silkworm, *Bombyx mori*. J. Proteome Res. 15: 1435–1445.

Fujii, T., T. Daimon, K. Uchino, Y. Banno, S. Katsuma, H. Sezutsu, T. Tamura, and T. Shimada. 2010. Transgenic analysis of the *BmBLOS2* gene that governs the translucency of the larval integument of the silkworm, *Bombyx mori*. Insect Mol. Biol. 19: 659–667.

Fujii, T., Y. Banno, H. Abe, S. Katsuma, and T. Shimada. 2012. A homolog of the human Hermansky-Pudluck syndrome-5 (HPS5) gene is responsible for the oa larval translucent mutants in the silkworm, *Bombyx mori*. Genetica. 140: 463–468.

Fujii, T., H. Abe, M. Kawamoto, S. Katsuma, Y. Banno, and T. Shimada. 2013. Albino (*al*) is a tetrahydrobiopterin (BH4)-deficient mutant of the silkworm *Bombyx mori*. Insect Biochem. Mol. Biol. 43: 594–600.

Fujii, T., K. Yamamoto, and Y. Banno. 2016. Molybdenum cofactor deficiency causes translucent integument, male-biased lethality, and flaccid paralysis in the silkworm *Bombyx mori*. Insect Biochem. Mol. Biol. 73: 20–26.

Futahashi, R., S. Okamoto, H. Kawasaki, Y. S. Zhong, M. Iwanaga, K. Mita, and H. Fujiwara. 2008. Genome-wide identification of cuticular protein genes in the silkworm, *Bombyx mori*. Insect Biochem. Mol. Biol. 38: 1138–1146.

Futahashi, R., Y. Banno, and H. Fujiwara. 2010. Caterpillar color patterns are determined by a two-phase melanin gene prepatterning process: new evidence from *tan* and *laccase2*. Evol. Dev. 12: 157–167.

Futahashi, R., H. Shirataki, T. Narita, K. Mita, and H. Fujiwara. 2012. Comprehensive microarray-based analysis for stage-specific larval camouflage pattern-associated genes in the swallowtail butterfly, *Papilio xuthus*. BMC Biol. 10: 46.

Guan, X., B. W. Middlebrooks, S. Alexander, and S. A. Wasserman. 2006. Mutation of TweedleD, a member of an unconventional cuticle protein family, alters body shape in *Drosophila*. Proc. Natl. Acad. Sci. USA 103: 16794–16799.

Hu, Y. G., Y. H. Shen, Z. Zhang, and G. Q. Shi. 2013. Melanin and urate act to prevent ultraviolet damage in the integument of the silkworm, *Bombyx mori*. Arch. Insect Biochem. Physiol. 83: 41–55.

Ito, K., S. Katsuma, K. Yamamoto, K. Kadono-Okuda, K. Mita, and T. Shimada. 2009. A 25bp-long insertional mutation in the *BmVarp* gene causes the *waxy* translucent skin of the silkworm, *Bombyx mori*. Insect Biochem. Mol. Biol. 39: 287–293.

Ito, K., S. Katsuma, K. Yamamoto, K. Kadono-Okuda, K. Mita, and T. Shimada. 2010. Yellow-e determines the color pattern of larval head and tail spots of the silkworm *Bombyx mori*. J. Biol. Chem. 285: 5624–5629.

Ito, K., M. Yoshikawa, T. Fujii, H. Tabunoki, and T. Yokoyama. 2016. Melanin pigmentation gives rise to black spots on the wings of the silkworm *Bombyx mori*. J. Insect Physiol. 91–92: 100–106.

Janssen, J. M., A. Monteiro, and P. M. Brakefield. 2001. Correlations between scale structure and pigmentation in butterfly wings. Evol. Dev. 3: 415–423.

Kiuchi, T., Y. Banno, S. Katsuma, and T. Shimada. 2011. Mutations in an amino acid transporter gene are responsible for sex-linked translucent larval skin of the silkworm, *Bombyx mori*. Insect Biochem. Mol. Biol. 41: 680–687.

Kômoto, N. 2002. A deleted portion of one of the two xanthine dehydrogenase genes causes translucent larval skin in the oq mutant of the silkworm (*Bombyx mori*). Insect Biochem. Mol. Biol. 32: 591–597.

Kômoto, N., H. Sezutsu, K. Yukuhiro, Y. Banno, and H. Fujii. 2003. Mutations of the silkworm molybdenum cofactor sulfurase gene, og, cause translucent larval skin. Insect Biochem. Mol. Biol. 33: 417–427.

Kômoto, N., G. X. Quan, H. Sezutsu, and T. Tamura. 2009. A single-base deletion in an ABC transporter gene causes white eyes, white eggs, and translucent larval skin in the silkworm *w-3(oe)* mutant. Insect Biochem. Mol. Biol. 39: 152–156.

Letsou, A., S. Alexander, K. Orth, and S. A. Wasserman. 1991. Genetic and molecular characterization of tube, a *Drosophila* gene maternally required for embryonic dorsoventral polarity. Proc. Natl. Acad. Sci. USA. 88: 810–814.

Linares, G. R., W. Xing, K. E. Govoni, S. T. Chen, and S. Mohan. 2009. Glutaredoxin 5 regulates osteoblast apoptosis by protecting against oxidative stress. Bone. 44: 795–804.

Liu, C., K. Yamamoto, T. C. Cheng, K. Kadono-Okuda, J. Narukawa, S. P. Liu, Y. Han, R. Futahashi, K. Kidokoro, H. Noda, et al. 2010. Repression of tyrosine hydroxylase is responsible for the sex-linked chocolate mutation of the silkworm, *Bombyx mori*. Proc. Natl. Acad. Sci. USA. 107: 12980–12985.

Luber, C. A., J. Cox, H. Lauterbach, B. Fancke, M. Selbach, J. Tschopp, S. Akira, M. Wiegand, H. Hochrein, M. O'Keeffe, et al. 2010. Quantitative proteomics reveals subset-specific viral recognition in dendritic cells. Immunity. 32: 279–289.

Luschnig, S., T. Bätz, K. Armbruster, and M. A. Krasnow. 2006. serpentine and *vermiform* encode matrix proteins with chitin binding and deacetylation domains that limit tracheal tube length in *Drosophila*. Curr. Biol. 16: 186–194.

Moussian, B., H. Schwarz, S. Bartoszewski, and C. Nüsslein-Volhard. 2005a. Involvement of chitin in exoskeleton morphogenesis in *Drosophila melanogaster*. J. Morphol. 264: 117–130.

Moussian, B., J. Söding, H. Schwarz, and C. Nüsslein-Volhard. 2005b. Retroactive, a membrane-anchored extracellular protein related to vertebrate snake neurotoxin-like proteins, is required for cuticle organization in the larva of *Drosophila melanogaster*. Dev. Dyn. 233: 1056–1063.

Ninomiya, Y., K. Tanaka, and Y. Hayakawa. 2006. Mechanisms of black and white stripe pattern formation in the cuticles of insect larvae. J. Insect Physiol. 52: 638–645.

Ostrowski, S., H. A. Dierick, and A. Bejsovec. 2002. Genetic control of cuticle formation during embryonic development of *Drosophila melanogaster*. Genetics 161: 171–182.

Pérez, V., D. López, E. Boixadera, M. Ibernón, A. Espinal, J. Bonet, and R. Romero. 2017. Comparative differential proteomic analysis of minimal change disease and focal segmental glomerulosclerosis. BMC Nephrol. 18: 49.

Qiao, L., G. Xiong, R. X. Wang, S. Z. He, J. Chen, X. L. Tong, H. Hu, C. L. Li, T. T. Gai, Y. Q. Xin, et al. 2014. Mutation of a cuticular protein, *BmorCPR2*, alters larval body shape and adaptability in silkworm, *Bombyx mori*. Genetics 196: 1103–1115.

Qiu, F., S. Brendel, P. M. Cunha, N. Astola, B. Song, E. E. Furlong, K. R. Leonard, and B. Bullard. 2005. Myofilin, a protein in the thick filaments of insect muscle. J. Cell Sci. 118: 1527–1536.

Qu, M., Y. Ren, Y. Liu, and Q. Yang. 2017. Studies on the chitin/chitosan binding properties of six cuticular proteins analogous to peritrophin 3 from *Bombyx mori*. Insect Mol. Biol. 26: 432–439.

Schwanhäusser, B., D. Busse, N. Li, G. Dittmar, J. Schuchhardt, J. Wolf, W. Chen, and M. Selbach. 2011. Global quantification of mammalian gene expression control. Nature. 473: 337–342.

Sun, X. J., B. Wu, L. Q. Zhou, Z. H. Liu, Y. H. Dong, and A. G. Yang. 2017. Isolation and characterization of melanin pigment from Yesso scallop *Patinopecten yessoensis*. J Ocean Univ China. 16: 279–284.

Tajiri, R. 2017. Cuticle itself as a central and dynamic player in shaping cuticle. Curr. Opin. Insect Sci. 19: 30–35.

Tajiri, R., N. Ogawa, H. Fujiwara, and T. Kojima. 2017. Mechanical control of whole body shape by a single cuticular protein obstructor-E in *Drosophila melanogaster*. Plos Genet. 13: e1006548.

Tamura, T. 1977. Deficiency in xanthine dehydrogenase activity in the *og* and *ogt* mutants of the silkworm, *Bombyx mori*. J. Seric. Sci. Jpn. 46: 113–119.

Tamura, T., and H. Akai. 1990. Comparative ultrastructure of larval hypodermal cell in normal and oily *Bombyx* mutants. Cytologia 55: 519–530.

Tamura, T., and S. Sakate. 1983. Relationship between expression of oily character and uric acid incorporation in the larval integument of various oily mutants of the silkworm, *Bombyx mori*. Bull. Seric. Exp. Sta. 28: 719–740.

Tonning, A., S. Helms, H. Schwarz, A. E. Uv, and B. Moussian. 2006. Hormonal regulation of *mummy* is needed for apical extracellular matrix formation and epithelial morphogenesis in *Drosophila*. Development 133: 331–341.

Vincent, J. F. V., and U. G. K. Wegst. 2004. Design and mechanical properties of insect cuticle. Arthropod Struct. Dev. 33: 187–199.

Wang, B., K. M. Sullivan, and K. Beckingham. 2003. Drosophila calmodulin mutants with specific defects in the musculature or in the nervous system. Genetics 165: 1255–1268.

Wang, L., T. Kiuchi, T. Fujii, T. Daimon, M. Li, Y. Banno, S. Katsuma, and T. Shimada. 2013a. Reduced expression of the *dysbindin*-like gene in the *Bombyx mori ov* mutant exhibiting mottled translucency of the larval skin. Genome 56: 101–108.

Wang, L., T. Kiuchi, T. Fujii, T. Daimon, M. Li, Y. Banno, S. Kikuta, T. Kikawada, S. Katsuma, and T. Shimada. 2013b. Mutation of a novel ABC transporter gene is responsible for the failure to incorporate uric acid in the epidermis of *ok* mutants of the silkworm, *Bombyx mori*. Insect Biochem. Mol. Biol. 43: 562–571.

Wiśniewski, J. R., A. Zougman, N. Nagaraj, and M. Mann. 2009. Universal sample preparation method for proteome analysis. Nat. Methods 6: 359–362.

Xiong, G., X. Tong, T. Gai, C. Li, L. Qiao, A. Monteiro, H. Hu, M. Han, X. Ding, S. Wu, et al. 2017. Body shape and coloration of silkworm larvae are influenced by a novel cuticular protein. Genetics 207: 1053–1066.

Yamaguchi, J., Y. Banno, K. Mita, K. Yamamoto, T. Ando, and H. Fujiwara. 2013. Periodic *Wnt1* expression in response to ecdysteroid generates twin-spot markings on caterpillars. Nat. Commun. 4: 1857.

Yoda, S., J. Yamaguchi, K. Mita, K. Yamamoto, Y. Banno, T. Ando, T. Daimon, and H. Fujiwara. 2014. The transcription factor Apontic-like controls diverse colouration pattern in caterpillars. Nat. Commun. 5: 4936.

Yoshimura, R., H. Doira, and K. Shinkura. 1984. Genetical studies on the "Dominant obese translucent" mutation in the silkworm, *Bombyx mori*. J. Seric. Sci. Jpn. 53: 348–351.

Yuasa, M., T. Kiuchi, Y. Banno, S. Katsuma, and T. Shimada. 2016. Identification of the silkworm *quail* gene reveals a crucial role of a receptor guanylyl cyclase in larval pigmentation. Insect Biochem. Mol. Biol. 68: 33–40.

Zhan, S., Q. Guo, M. Li, M. Li, J. Li, X. Miao, and Y. Huang. 2010. Disruption of an N-acetyltransferase gene in the silkworm reveals a novel role in pigmentation. Development 137: 4083–4090.

Zhang, J. Z., and K. Y. Zhu. 2006. Characterization of a chitin synthase cDNA and its increased mRNA level associated with decreased chitin synthesis in *Anopheles quadrimaculatus* exposed to diflubenzuron. Insect Biochem. Mol. Biol. 36: 712–725.

Zhang, H., T. Kiuchi, L. Wang, M. Kawamoto, Y. Suzuki, S. Sugano, Y. Banno, S. Katsuma, and T. Shimada. 2017. *Bm-muted*, orthologous to mouse muted and encoding a subunit of the BLOC-1 complex, is responsible for the otm translucent mutation of the silkworm *Bombyx mori*. Gene 629: 92–100.

Zhu, K. Y., H. Merzendorfer, W. Zhang, J. Zhang, and S. Muthukrishnan. 2016. Biosynthesis, turnover, and functions of chitin in insects. Annu. Rev. Entomol. 61: 177–196.